

International Journal of Biological and Natural Sciences

ISSN 2764-1813

vol. 6, n. 1, 2026

... ARTICLE 11

Acceptance date: 09/04/2026

SIMULATION OF THE POPULATION DYNAMICS OF *DIAPHORINA CITRI* IN CITRUS TREES UNDER PHENOLOGICAL, CLIMATIC, AND IMMIGRATION STRESS

Ramírez-Ramírez Faustino

National Technological Institute of Mexico, Tlajomulco Campus, Jal., Doctor of Science in Biotechnology in Agricultural Processes. Tlajomulco-San Miguel Cuyutlán Highway. Tlajomulco de Zúñiga, Jal.

Chávez-Rodríguez Arturo Moisés

National Technological Institute of Mexico, Tlajomulco Campus, Jal., Doctor of Science in Biotechnology in Agricultural Processes. Tlajomulco-San Miguel Cuyutlán Highway. Tlajomulco de Zúñiga, Jal.
Corresponding author

Andrade-González Isaac

National Technological Institute of Mexico, Tlajomulco Campus, Jal., Doctor of Science in Biotechnology in Agricultural Processes. Tlajomulco-San Miguel Cuyutlán Highway. Tlajomulco de Zúñiga, Jal.



All content published in this journal is licensed under the Creative Commons Attribution 4.0 International License (CC BY 4.0).

Fariás-Cervantes Vania Sbeyde

National Technological Institute of Mexico, Tlajomulco Campus, Jal., Doctor of Science in Biotechnology in Agricultural Processes. Tlajomulco-San Miguel Cuyutlán Highway. Tlajomulco de Zúñiga, Jal.

Montero-Cortés Mayra Itzcalotzin

National Technological Institute of Mexico, Tlajomulco Campus, Jal., Doctor of Science in Biotechnology in Agricultural Processes. Tlajomulco-San Miguel Cuyutlán Highway. Tlajomulco de Zúñiga, Jal.

Flores-Benítez Silvia

National Technological Institute of Mexico, El Llano Campus, Aguascalientes, Division of Graduate Studies and Research. , Aguascalientes-San Luis Potosí Highway, El Llano, Aguascalientes

Hernández-Monreal Diana

National Technological Institute of Mexico, Tlajomulco Campus, Jal., Doctor of Science in Biotechnology in Agricultural Processes. Tlajomulco-San Miguel Cuyutlán Highway. Tlajomulco de Zúñiga, Jal.

Abstract: *Diaphorina citri* Kuwayama is the primary vector of huanglongbing, and its temporal dynamics depend on the interaction between host budbreak, climate, and spatial connectivity. The objective of this study was to simulate the weekly population dynamics of *D. citri* in citrus trees under phenological, climatic, and external immigration forcing using a discrete-event model structured into eggs, nymphs, and adults. A mechanistic system was implemented in SAS with a 52-week horizon, parameterized with weekly mortalities of 0.20 for eggs and nymphs, 0.10 for adults, emigration of 0.05, and a baseline oviposition rate of 50 eggs per adult per week. The phenological signal ranged from 0.55 to 1.55, while external immigration varied between 1 and 7 adult equivalents per week. Adjusted oviposition increased from 12.60 in January to 85.25 in July. The simulation reproduced an initial establishment phase, followed by a marked acceleration starting in February and a peak expansion between June and August, when high phenology, average temperatures of 24.7–26.9 °C, and increased immigration coincided. In week 32, the population reached 2.78×10^{15} eggs, 7.56×10^{14} nymphs, and 1.11×10^{14} adults. At the end of the period, the values were 4.06×10^{22} , 1.73×10^{22} , and 4.41×10^{21} , respectively. These results indicate that the synchronization between hatching, climate, and immigration decisively reorganizes the vector's growth rate and shifts the greatest population acceleration toward the spring–summer window. The final magnitude of the trajectories reflects the system's growth potential under favorable conditions, rather than literal local abundance, due to the absence of explicit mechanisms of demographic regulation.

Keywords: *Diaphorina citri*; population dynamics; citrus

Introduction

Diaphorina citri Kuwayama plays a central role in modern citrus cultivation due to its close association with young shoots, its ability to sustain populations throughout much of the year, and its role as a vector of huanglongbing. In terms of production, the insect's relevance depends not only on its presence but also on the speed with which it reorganizes its age structure when susceptible host tissue, a favorable environment, and spatial connectivity between orchards coincide. This combination makes the vector's temporal dynamics a critical component for surveillance, management scheduling, and the development of prospective scenarios in regional citrus systems (Leong et al., 2021; Ebert et al., 2023; Liu et al., 2024; Hernández et al., 2025).

The host's phenology is the most consistent biological determinant of these dynamics. In commercial citrus, the highest abundance of *D. citri* occurs during active budbreak, when young tissue concentrates oviposition, the establishment of immature stages, and adult aggregation. In Valencia oranges and Italian lemons, the seasonal abundance of the psyllid was directly associated with crop phenology, whereas in commercial orchards, the cyclic production of new flushes increased the abundance and aggregation of adults. This relationship between sprouting and population growth also aligns with the insect's biology at the physiological level, given that development, survival, and fecundity change markedly with temperature and define windows of greater demographic fitness (Álvarez-Ramos

et al., 2022; Leong et al., 2021; Liu & Tsai, 2000).

Building on this biological foundation, recent predictive approaches have shown that the temporal signal of *D. citri* arises from the interaction between biotic and abiotic variables. Machine learning-based models improved the prediction of eggs, nymphs, and adults when they simultaneously incorporated temperature, rainfall, and host phenological patterns, while weekly climate models demonstrated useful predictive capacity for anticipating psyllid abundance based on regional meteorological variables. The conceptual implication of these studies is clear: the vector population does not respond to a single factor, but rather to a forcing structure in which phenology, climate, and the system's temporal dynamics act in a coupled manner (Bibi et al., 2021; Singh et al., 2024; Bibi et al., 2026).

Despite this progress, a gap remains between studies of seasonal abundance, data-driven predictive models, and the latest mathematical developments. Field studies have precisely defined the relationship between budbreak and psyllid abundance, and predictive approaches have improved the ability to anticipate their temporal variation; however, much of recent modeling has focused on huanglongbing transmission, optimal control, or time-dependent stochastic systems, where the vector population is typically represented as an aggregated seasonal signal or as a subcomponent within a broader epidemiological framework. This trend has left less attention paid to a mechanistic population formulation of the psyllid in open landscapes, incorporating biological states, variable bud break, seasonal climate, and explicit external immigration (Cardo-

na-Salgado et al., 2025; Hernández et al., 2025; Liu et al., 2024; Xie et al., 2025).

In this context, this study was designed to simulate the weekly population dynamics of *D. citri* in citrus trees using a discrete-time model structured into eggs, nymphs, and adults, driven by host phenology, seasonal climate, and external immigration. The central premise was that the synchronization between peak budbreak, favorable environmental conditions, and the continuous influx of adults from the perimeter reorganizes the system's growth rate and shifts the greatest population acceleration toward the spring–summer window. From this perspective, the objective was to construct a mechanistic baseline capable of describing the intrinsic behavior of the vector under conditions favorable for its development, identifying the time window of greatest population acceleration, and providing a conceptual platform for future extensions involving demographic regulation, spatial heterogeneity, and time-dependent management modules (Álvarez-Ramos et al., 2022; Bibi et al., 2021; Singh et al., 2024; Cardona-Salgado et al., 2025).

Materials and Methods

General Structure of the Model

A discrete-time model with weekly intervals was formulated to describe the population dynamics of *Diaphorina citri* in an open citrus system, with three state variables: eggs, nymphs, and adults. The simulation spanned 52 weeks, with initial conditions, and was designed to represent the insect's response under variable flush regimes, seasonal climate, and external immigration. The approach was constructed

as a mechanistic population model, without infection compartments, to capture the biological sequence of egg laying, immature development, adult emergence, and entry of individuals from the system's edge. This timescale is consistent with studies of seasonal abundance, flushing cycles, and weekly predictive models of the citrus psyllid, where the host's and environment's phenological signals explain much of the observed population variation (Álvarez-Ramos et al., 2022; Leong et al., 2021; Bibi et al., 2021; Singh et al., 2024).

The weekly system update was defined by the following equations:

$$E_t = (1 - \mu_E)(1 - \gamma_{E,t})E_{t-1} + \beta_t A_{t-1}$$

$$N_t = (1 - \mu_N)(1 - \gamma_{N,t})N_{t-1} + (1 - \mu_E)\gamma_{E,t}E_{t-1}$$

$$A_t = (1 - \mu_A - \delta)A_{t-1} + (1 - \mu_N)\gamma_{N,t}N_{t-1} + \Lambda_t$$

where μ_E , μ_N , and μ_A correspond to the weekly mortality rates of eggs, nymphs, and adults; and β_t , $\gamma_{E,t}$, and $\gamma_{N,t}$ represent the weekly transition probabilities between states; δ is the weekly emigration of adults from the spatial unit; Λ_t is the adjusted weekly oviposition; and δ is the weekly external immigration. This formulation focused on the insect's demographic behavior under conditions favorable for its development and reproduction, that is, under a scenario that reflects the biological system's natural growth potential when a suitable host, a favorable environment, and spatial connectivity coincide.

Biological parameters

The biological parameters were obtained from the literature and incorporated into the model as fixed reference values. Weekly mortality of eggs and nymphs was set at $\mu_E=0.20$ and $\mu_N=0.20$, while we-

ekly mortality of adults was set at $\mu_A=0.10$, in accordance with the psyllid's response to temperature described by Liu and Tsai. Weekly adult emigration was set at $\delta=0.05$, consistent with evidence of seasonal flight activity and adult movement in open citrus orchards reported by Hall and Hentz. Basal oviposition was set at $\beta_{\text{base}}=50$ eggs per adult per week as an operational value derived from fertility literature for *D. citri* and used in the script as the baseline condition under favorable environmental conditions (Wenninger & Hall, 2007; Liu & Tsai, 2000; Hall & Hentz, 2011).

The average duration of the egg stage was determined to be 3.00 days, and the duration of the nymphal stage was determined to be 12.41 days. These values were derived from an average egg-to-adult development time of 15.41 days, documented for *D. citri* under greenhouse conditions with a maximum temperature of 37.1 °C, a minimum temperature of 25.0 °C, a maximum relative humidity of 67.0%, a minimum relative humidity of 39.5%, and a photoperiod of 12:12 h. From these durations, the weekly baseline transition probabilities $\gamma_{(E,\text{base})}=0.9030$ and $\gamma_{(N,\text{base})}=0.4311$ were derived, with the aim of maintaining consistency between development times and weekly population turnover (García et al., 2016; Liu & Tsai, 2000).

Phenological, climatic, and immigration drivers

The host's phenology was represented by a weekly coefficient ($F_{\text{fen},t}$) with values ranging from 0.55 to 1.55, assigned to replicate an annual pattern of low bud break in winter, a gradual increase from late winter, peaks between June and August, and a subsequent decline in autumn. This scheme

was based on field evidence showing that *D. citri* is most abundant during active flushing phases, as well as the positive relationship between flushing cycles and the presence of eggs, nymphs, and adults on commercial citrus trees (Álvarez-Ramos et al., 2022; Leong et al., 2021).

The climate component was constructed using an estimated monthly time series for 2014–2023 in Autlán de Navarro, Jalisco, derived from 1991–2023 climate data and local annual trends. For each month, an estimated mean temperature, estimated precipitation, and a rainfall index normalized relative to the rainiest month of the year were assigned. These monthly values were applied to each week according to the simulation calendar. Based on this, a thermal factor and a rainfall factor $F_{\text{fen},t}$ and a rainfall factor $F_{\text{lluv},t}$ were defined, used to modulate oviposition and, in the case of temperature, also the transition rate between states. The explicit inclusion of temperature and rainfall as drivers followed the same criteria used in recent predictive models of *D. citri*, where weekly temperature, rainfall, and phenological predictors improve the temporal explanation of eggs, nymphs, and adults (Bibi et al., 2021; Singh et al., 2024).

External immigration was defined as $\Lambda_t = \lambda_0 \times \kappa \times I_{\text{borde},t}$, where $\lambda_0=1.0$ represented the weekly baseline influx calibrated from edge sampling, $\kappa=1.0$ was the conversion factor from captures to adult equivalents, and $I_{\text{borde},t}$ was the weekly edge capture index. In the script, this index ranged from 1 to 7 to represent relative variation in adult influx throughout the year. The use of an immigration term was based on evidence of seasonal movement of the psyllid in orchards and adjacent areas, where flight activity changes throughout the year and helps

maintain connectivity between crop units (Hall & Hentz, 2011).

Functional parameterization of the script

For each week, the adjusted oviposition was calculated as:

$$\beta_t = \beta_{base} \times F_{fen,t} \times F_{temp,t} \times F_{iluv,t}$$

In this way, reproduction was controlled by the host's phenological quality and the environmental suitability of the weekly period. The transition probabilities between states were adjusted based on the weekly thermal factor:

$$\gamma_{E,t} = \gamma_{E,base} \times F_{temp,t}$$

$$\gamma_{N,t} = \gamma_{N,base} \times F_{temp,t}$$

This design assumed that phenology and the environment directly affect the insect's oviposition capacity, while temperature also modifies the relative rate of development. The available literature on *D. citri* supports this framework, given that egg laying is concentrated on young shoots and the insect's development varies with temperature and host quality (Liu & Tsai, 2000; Álvarez-Ramos et al., 2022; Bibi et al., 2021).

Implementation in SAS

The simulation was implemented in SAS using an iterative routine spanning 53 time steps, from week 0 to week 52. Datasets were generated for parameters, monthly climate, weekly forcings, key-week summaries, and the full simulation. In each iteration, E_t , N_t , and A_t were updated using the

values from the previous week and the forcings corresponding to the current week. The script's outputs included the complete time series for eggs, nymphs, and adults, as well as tables grouped by time blocks and multiple-series graphs to describe the system's annual trajectory.

Biological significance and interpretation of the results

The model was deliberately designed as an open system under conditions favorable to the insect's natural behavior, featuring high baseline fertility, relatively low mortality rates, low emigration, peak phenology between June and August, and positive external immigration. Under this combination, the model's structure favors very strong cumulative growth, because each cohort feeds the next without any internal mechanism for population saturation. Consequently, obtaining values in the range of 10^{20} to 10^{22} at the end of the simulation is mathematically consistent with the formulation used, since the system accumulates reproduction, transition, and external input week after week. This output should be interpreted as an expression of the insect's growth potential under favorable conditions, rather than as a literal local abundance or as a density directly applicable to field populations or trap catches.

For this reason, the model's objective was not to estimate realistic absolute values of local abundance, but rather to identify the time window of maximum population growth and to describe how the synchronization between budding, climate, and immigration reshapes the vector's demographic trajectory. The absence of carrying capacity, density dependence, predation, host depletion, or induced control allows us to

visualize the intrinsic behavior of the system under conditions favorable to *D. citri*. This approach serves as a mechanistic baseline for subsequent extensions involving population regulation, spatial heterogeneity, or management modules, as seen in more complex dynamic models of the vector or the associated citrus system (Cardona-Salgado et al., 2025; Liu et al., 2024; Xie et al., 2025; Hernández et al., 2025).

Results and Discussion

Biological parameters of the model

The biological structure was defined by a baseline weekly egg-laying rate of 50.0000 eggs per adult, a mortality rate of 0.2000 among eggs and nymphs, a mortality rate of 0.1000 among adults, an additional loss due to dispersion of 0.0500, and baseline transition probabilities of 0.9030 from the egg stage to the nymphal stage, and 0.4311 from the nymphal stage to the adult stage (Table 1). The assumed average duration of 3.00 days for eggs and 12.41 days for nymphs placed the model in a regime of rapid inter-weekly turnover, with a structural predominance of immature stages from the initial formulation.

Under this parameterization, the system's growth was driven by high fecundity relative to loss rates, such that the accumulation of eggs constituted the first stage of expansion, and the increase in nymphs and adults emerged as a staggered consequence of ontogenetic turnover. This behavior is consistent with the biology of *Diaphorina citri* described by Liu and Tsai, who documented that development, survival, and life table parameters change markedly with temperature, and with subsequent predicti-

ve approaches that treat eggs, nymphs, and adults separately due to their differential response to temperature, rainfall, and host phenology (Liu & Tsai, 2000; Bibi et al., 2021; Singh et al., 2024). The relevance of maintaining this separation by life stage also aligns with more recent population models that explicitly represent the psyllid's biological structure, whether through mechanistic approaches or through machine learning with biotic and abiotic variables as joint predictors (Bibi et al., 2026; Cardona-Salgado et al., 2025; Xie et al., 2025).

The combination of high fecundity, rapid development from the egg stage, and relatively low adult mortality thus established a biological framework for describing the vector's weekly growth potential when the system is subjected to favorable environmental conditions. This mechanistic core is consistent with studies of temporal abundance in citrus, where egg-laying and immature development pulses precede the increase in the adult fraction and explain the stepped pattern of annual dynamics (Álvarez-Ramos et al., 2022; Leong et al., 2021).

Immigration Parameters

The immigration signal was set at a baseline weekly inflow of 1.0000 adult equivalents and a unit conversion factor between edge captures and adults entering the system, thereby leaving local dynamics open to external flow from the surrounding landscape (Table 2).

The inclusion of $\lambda_0 = 1.0000$ and $\kappa = 1.0000$ meant that the population trajectory did not depend exclusively on internal reproduction, but also on the continuous influx of adults from the edge of the orchard. This structure is consistent with the

Parametros biologicos del modelo

Parametro	Descripcion	Fuente	Valor
beta_base	Oviposicion basal semanal por adulto bajo condiciones favorables	Base del modelo	50.0000
muE	Mortalidad semanal de huevos	Liu y Tsai (2000)	0.2000
muN	Mortalidad semanal de ninfas	Liu y Tsai (2000)	0.2000
muA	Mortalidad semanal de adultos	Liu y Tsai (2000)	0.1000
delta	Emigracion o dispersion semanal de adultos fuera de la unidad espacial	Supuesto operativo del modelo	0.0500
dur_huevo_dias	Duracion media asumida del estado de huevo	Ajuste biologico	3.0000
dur_ninfa_dias	Duracion media del estado ninfal agrupado	15.41 dias huevo-adulto menos 3 dias de huevo	12.4100
gammaE_base	Probabilidad semanal basal de transicion huevo->ninfa	Derivada de duracion biologica	0.9030
gammaN_base	Probabilidad semanal basal de transicion ninfa->adulto	Derivada de duracion biologica	0.4311

Table 1. Biological parameters of the model

Sources: SAS Studio 2026

Parametros de migracion calibrados desde muestreo de borde

Parametro	Descripcion	Fuente	Valor
lambda0	Ingreso basal semanal calibrado desde muestreo de borde en baja brotacion	Mediana robusta del muestreo de borde	1.0000
kappa	Factor de conversion de capturas a adultos equivalentes	Supuesto operativo del modelo	1.0000

Table 2. Immigration parameters calibrated from edge sampling.

Sources: SAS Studio 2026

Resumen de la simulacion en semanas clave

Semana	Fecha	Mes	Periodo	Fenologia	Temp media (°C)	Precipitacion estimada (mm)	Indice lluvia	Capturas borde	Lambda(t)	Beta(t)	GammaE(t)	GammaN(t)	Huevos (E)	Ninfas (N)	Adultos (A)
0	01JAN2024	Enero	Inicial	0.60	21.7955	33.7171	0.1829	1	1.0000	12.6000	0.5418	0.2587	100.00	50.00	20.00
4	21JAN2024	Enero	Baja_brotacion	0.60	21.7955	33.7171	0.1829	1	1.0000	12.6000	0.5418	0.2587	1325.91	549.82	144.00
8	18FEB2024	Febrero	Alta_brotacion	1.10	22.5955	25.2878	0.1371	2	2.0000	32.7250	0.7676	0.3964	34167.79	13361.96	2560.13
12	17MAR2024	Marzo	Alta_brotacion	1.20	23.9955	13.6976	0.0743	3	3.0000	35.7000	0.7676	0.3964	1227344.65	409562.93	79434.81
16	14APR2024	Abril	Alta_brotacion	1.15	25.7955	2.1073	0.0114	3	3.0000	40.2500	0.9030	0.4311	49399183.25	16117326.30	3195489.22
20	12MAY2024	Mayo	Alta_brotacion	1.30	26.8955	12.6439	0.0686	4	4.0000	45.5000	0.9030	0.4311	2733916480.27	874915540.56	153227605.02
24	09JUN2024	Junio	Alta_brotacion	1.55	25.9955	131.7073	0.7143	6	6.0000	77.5000	0.9030	0.4311	252943512964.94	7546077785.99	8714912754.10
28	07JUL2024	Julio	Alta_brotacion	1.55	24.7955	184.3903	1.0000	7	7.0000	85.2500	0.9030	0.4311	25788383704288.70	6924965757807.00	1004097425381.38
32	04AUG2024	Agosto	Alta_brotacion	1.45	24.6955	152.7805	0.8286	5	5.0000	79.7500	0.9030	0.4311	2778894564816139.00	756482840730763.00	110915429072230.00
36	01SEP2024	Septiembre	Baja_brotacion	0.95	24.4955	155.9415	0.8457	3	3.0000	44.4125	0.7676	0.3964	175600174866296628.0	86274071381191128.00	10200640596890380.00
40	29SEP2024	Septiembre	Baja_brotacion	0.95	24.4955	155.9415	0.8457	3	3.0000	44.4125	0.7676	0.3964	7912846168202360832	2479234786206694912	440718342314110080.0
44	27OCT2024	Octubre	Baja_brotacion	0.75	24.5955	82.1854	0.4457	2	2.0000	31.8750	0.7676	0.3964	2.0943880594167E20	72822139662857396224	13834416351664381952
48	24NOV2024	Noviembre	Baja_brotacion	0.60	23.5955	26.3415	0.1429	1	1.0000	17.8500	0.7676	0.3964	2.7974963472938E21	1.1809670101668E21	2.7453834930353E20
52	22DEC2024	Diciembre	Baja_brotacion	0.55	22.2955	15.8049	0.0857	1	1.0000	16.3625	0.7676	0.3964	4.0615940878629E22	1.7295500910549E22	4.4126204904581E21

Table 3. Summary of the simulation for key weeks.

Sources: SAS Studio 2026

psyllid's spatial ecology, as adult aggregation, movement, and persistence within the crop intensify during the production cycles of young shoots. In commercial orchards, the increase in *D. citri* abundance has been described as a response closely linked to flush cycles, with greater aggregation and dispersal of adults when new shoots are generated, such that external immigration acts as an ecologically consistent component of the model (Leong et al., 2021).

The role of the edge also aligns with the regional variation in seasonal abundance described in citrus crops. Álvarez-Ramos et al. documented differences between areas and between crops with varying continuity of budding, suggesting that the local vector population responds to a spatially heterogeneous environment rather than a closed system. Along the same lines, Cardona-Salgado et al. showed that the trajectory of *D. citri* changes when population dynamics incorporate fine-scale biological structure and temporal control, reinforcing the need to explicitly account for the external influx of individuals when modeling an open landscape (Álvarez-Ramos et al., 2022; Cardona-Salgado et al., 2025).

Model drivers

The annual forcing signal combined a clear phenological gradient, a favorable thermal environment for most of the year, and increased immigration from outside between June and August. This synchrony reorganized the weekly magnitude of $\lambda(t)$, $\beta(t)$, $\gamma_E(t)$, and $\gamma_N(t)$, and was directly reflected in the temporal progression of eggs, nymphs, and adults. The transition from an initial phase of low hatching to a phase of high hatching was summarized

In January, with a phenology value of 0.60, $\lambda(t) = 1.0000$, and $\beta(t) = 12.6000$, the population remained in an establishment phase, with 1,325.91 eggs, 549.82 nymphs, and 144.00 adults in week 4. In February and March, the rise in phenology to 1.10–1.20 and the increase in $\lambda(t)$ to 2.0000–4.0000 shifted the trajectory toward a rapid acceleration phase, reaching 1.23×10^6 eggs, 4.10×10^5 nymphs, and 7.94×10^4 adults in week 12. The system's peak momentum was concentrated between June and August, when phenology of 1.45–1.55, $\lambda(t)$ of 5.0000–7.0000, $\beta(t)$ between 77.5000 and 85.2500, and average temperatures near 24.7–26.0 °C coincided; under this configuration, the simulation reached 2.78×10^{15} eggs, 7.56×10^{14} nymphs, and 1.11×10^{14} adults in week 32. The temporal sequence aligns with field studies and population prediction models that identify the largest increases in *D. citri* during periods of active budding and under favorable weather conditions, with major peaks associated with the availability of young tissue and regional climate (Álvarez-Ramos et al., 2022; Leong et al., 2021; Singh et al., 2024; Bibi et al., 2021; Bibi et al., 2026).

Starting in September, the phenology index dropped to 0.95, then to 0.75 in October, and finally to 0.55–0.60 around November and December, but the population continued to grow. This persistence indicates strong demographic memory, resulting from the intergenerational accumulation of cohorts during spring and summer. The subsequent reduction in $\beta(t)$ and $\lambda(t)$ decreased the intensity of the forcing, but did not negate the cumulative effect of the immature mass already generated. This behavior is consistent with population and predictive models where the final response of the

vector depends on the temporal interaction between biotic and abiotic variables, not on a single isolated forcing factor (Bibi et al., 2021; Singh et al., 2024; Bibi et al., 2026).

The complete simulation from 0 to 52 weeks can be presented in a table organized by time blocks, preserving the annual sequence without overly fragmenting the manuscript (Table 4).

The condensed form confirms a six-phase pattern: winter establishment, late-winter acceleration, spring expansion, peak amplification in summer, and autumn-winter persistence sustained by population inertia. This temporal structure aligns well with the psyllid's phenology as described in studies of seasonal abundance and with recent approaches where predictive performance improves by integrating climate, budbreak, and other biotic predictors. It also links methodologically with dynamic vector-plant system models that incorporate seasonal fluctuations, time-dependent control, or parameter optimization, as all of these recognize that the temporal signal of the adult component reorganizes the overall trajectory of the system (Ebert et al., 2023; Hernández et al., 2025; Liu et al., 2024; Xie et al., 2025).

Weekly population dynamics of *Diaphorina citri* in open landscapes

The weekly trend maintained the sequence eggs > nymphs > adults throughout the year and showed a marked change in slope beginning in February, followed by a phase of very intense growth between April and August. The egg population rose from 100.00 in week 0 to 4.0616×10^{22} in week 52; the nymph population, from 50.00 to 1.7296×10^{22} ; and the adult population, from 20.00 to 4.4126×10^{21} , indicating a

stepwise amplification of the reproductive signal across the three biological stages (Figure 1).

The initial increase in eggs preceded the subsequent expansion of nymphs and adults, so the figure clearly summarizes a coherent biological sequence: first, egg-laying intensified; then, the immature population increased; and finally, the adult population expanded. This progression is consistent with the behavior of *D. citri* in the field, where the availability of tender shoots triggers oviposition and pre-imaggo development, while adult abundance reflects the cumulative effect of state transitions and the persistence of phenological and climatic forcing (Álvarez-Ramos et al., 2022; Leong et al., 2021; Bibi et al., 2021; Singh et al., 2024).

The magnitude of the trajectory in the second half of the year also indicates that the current formulation captures with great sensitivity the synchrony between fecundity, transition, and external adult inflow. In terms of model structure, this result positions the adult fraction as the cumulative outcome of a system with a strong immature base and persistent seasonal forcing. This interpretation aligns well with Cardona-Salgado et al., who modeled the population dynamics of the psyllid with a detailed biological structure, and with the work of Hernández, Liu, and Xie, which demonstrates the need to introduce temporal control or structural constraints when the seasonal signal of the vector- s is sustainably coupled to the rest of the system. Ebert et al. further added that the adult fraction exhibits a marked seasonal organization at the population level, reinforcing the relevance of this phase as an integrator of the insect's annual dynamics (Cardona-Salgado et al., 2025; Ebert et al., 2023; Hernández et al., 2025; Liu et al., 2024; Xie et al., 2025).

Time block	Weeks	Phenology	$\lambda(t)$	$\beta(t)$	Eggs (start–end)	Nymphs (start–end)	Adults (start–end)
Early winter	0–5	0.55–0.60	1.0	12.6000– 16.3625	1.00×10^2 – 2.30×10^3	5.00×10^1 – 9.01×10^2	2.00×10^1 – 2.37×10^2
Late winter– early spring	6–14	1.10–1.20	2.0– 4.0	32.7250– 35.7000	8.19×10^3 – 7.27×10^6	1.87×10^3 – 2.37×10^6	4.68×10^2 – 4.41×10^5
Spring	15–22	1.15–1.30	3.0– 4.0	40.2500– 45.5000	1.83×10^7 – 2.02×10^{10}	6.33×10^6 – 6.27×10^9	1.19×10^6 – 1.19×10^9
Summer	23–35	1.45–1.55	5.0– 7.0	77.5000– 85.2500	$9.35 \times$ 10^{10} – 9.10 $\times 10^{16}$	1.75×10^{10} – 2.44×10^{16}	3.17×10^9 – 3.57×10^{15}
Early fall	36–44	0.75–0.95	2.0– 3.0	31.8750– 44.4125	$1.76 \times$ 10^{17} – 2.09 $\times 10^{20}$	6.83×10^{16} – 7.28×10^{19}	1.02×10^{16} – 1.38×10^{19}
Late fall–late winter	45–52	0.55–0.60	1.0	16.3625– 17.8500	$2.86 \times$ 10^{20} – 4.06 $\times 10^{22}$	1.66×10^{20} – 1.73×10^{22}	3.31×10^{19} – 4.41×10^{21}

Table. Complete simulation from 0 to 52 weeks condensed into time blocks.]

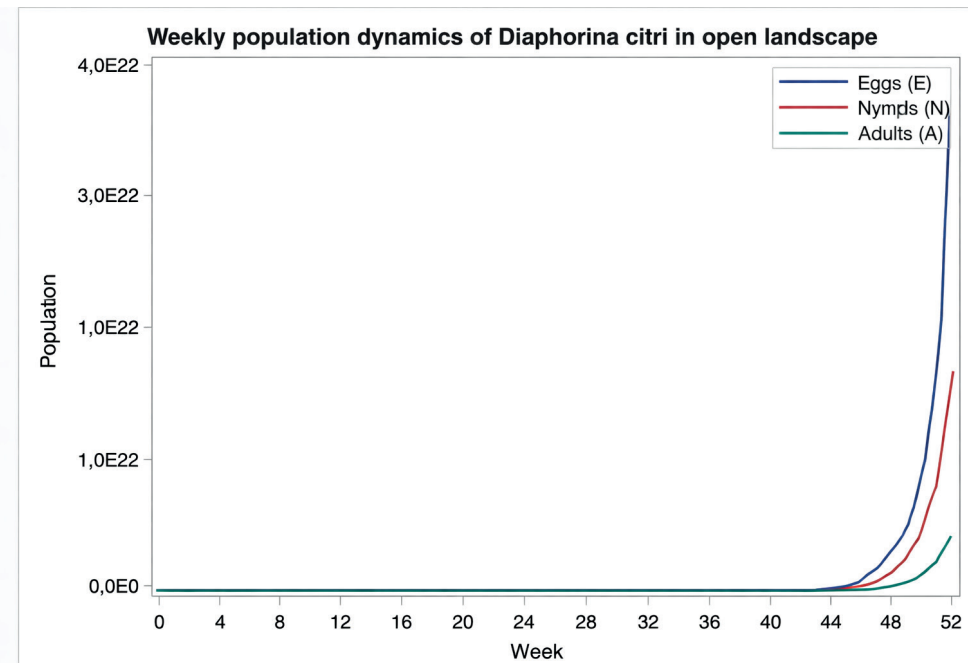


Figure 1. Weekly population dynamics of *Diaphorina citri* in open landscapes.

Sources: SAS Studio 2026

Conclusions

The simulation confirmed that the weekly population dynamics of *Diaphorina citri* on citrus trees were determined by the synchronization between host phenology, temperature, estimated precipitation, and external immigration, such that the greatest acceleration of the system occurred between spring and summer, when peak bud break, maximum adjusted oviposition rates, and the highest influx of adults from the perimeter coincided. Under this configuration, the model reproduced a coherent demographic sequence in which the increase in eggs preceded the accumulation of nymphs and, subsequently, the expansion of adults, as described for psyllid populations associated with the availability of tender shoots and with environmental conditions favorable for development and reproduction (Álvarez-Ramos et al., 2022; Leong et al., 2021; Liu & Tsai, 2000; Singh et al., 2024).

The biological framework used allowed for a mechanistic representation of the transition between life stages and the amplifying effect of high fecundity when the system operates within a favorable phenological and climatic window. The differentiated response of eggs, nymphs, and adults supported the appropriateness of modeling each life stage separately, because the forcing signal was not expressed with the same intensity across the entire population, but rather in a staggered and cumulative manner. This property aligns with recent prediction and machine learning approaches applied to *D. citri*, where the simultaneous inclusion of biotic and abiotic variables improves the explanation of the vector's temporal variation and allows for a more accurate capture of the internal structure of its annual dynamics (Bibi et al., 2021; Bibi et al., 2026; Singh et al., 2024).

The incorporation of a baseline immigration rate calibrated from edge sampling showed that the local population should be understood as an open system, influenced by the continuous flow of adults from the surrounding landscape. This component reinforced population expansion precisely during the periods of greatest phenological suitability of the crop, underscoring the importance of spatial context for interpreting vector pressure in commercial orchards and for designing spatially and temporally based surveillance schemes. From this perspective, the simulation not only identifies the annual window of greatest potential psyllid growth but also establishes a useful quantitative framework for scheduling intensive monitoring and management measures during periods when connectivity between the edge and the crop amplifies the population trajectory (Álvarez-Ramos et al., 2022; Leong et al., 2021; Cardona-Salgado et al., 2025).

The final magnitude of the simulated trajectories indicates that the current model clearly describes the vector's growth potential under sustained favorable forcing; however, the next methodological step requires incorporating processes that regulate population expansion, such as density dependence, carrying capacity, more explicit spatial heterogeneity, or time-dependent management modules. Such an expansion would enable the transformation of the current model into a tool with greater operational realism for prospective analyses and the comparison of intervention scenarios. On this basis, the present study provides a solid platform for subsequent research aimed at integrating temporal control, spatial landscape structure, and hybrid predictivity components into the population modeling of *D. citri* in regional citrus systems (Cardona-Salgado et al., 2025; Hernández et al., 2025; Liu et al., 2024; Xie et al., 2025).

References

- Álvarez-Ramos, R., Azuara-Domínguez, A., Rodríguez-Castro, J. H., Zavala-Zapata, V., Sánchez-Borja, M., & Vargas-Tovar, J. A. (2022). Abundancia estacional de *Diaphorina citri* asociada a la fenología del cultivo de cítricos. *Revista Mexicana de Ciencias Agrícolas*, 13(1), 89–101. <https://doi.org/10.29312/remexca.v13i1.2494>
- Bibi, M., Hanif, M. K., Sarwar, M. U., Khan, M. I., Khan, S. Z., Shivachi, C. S., Anees, A., & Ahmad, M. (2021). Monitoring population phenology of Asian citrus psyllid using deep learning. *Complexity*, 2021, 4644213. <https://doi.org/10.1155/2021/4644213>
- Bibi, M., Skarmeta, A. F., & Khan, S. Z. (2026). Monitoring population dynamics of Asian citrus psyllid-natural enemies using machine learning. *Smart Agricultural Technology*, 13, 101850. <https://doi.org/10.1016/j.attech.2026.101850>
- Cardona-Salgado, D., Dumont, Y., & Vasilieva, O. (2025). Natural population dynamics of Asian citrus psyllid, *Diaphorina citri*, and its control based on pheromone trapping. *Mathematical Biosciences*, 390, 109540. <https://doi.org/10.1016/j.mbs.2025.109540>
- Ebert, T. A., Shower, D., Brlansky, R. H., & Rogers, M. E. (2023). Seasonal patterns in the frequency of *Candidatus Liberibacter asiaticus* in populations of *Diaphorina citri* (Hemiptera: Psyllidae) in Florida. *Insects*, 14(9), 756. <https://doi.org/10.3390/insects14090756>
- García, Y., Ramos, Y. P., Sotelo, P. A., & Kondo, T. (2016). Biology of *Diaphorina citri* (Hemiptera: Liviidae) under glass house conditions in Palmira, Colombia. *Revista Colombiana de Entomología*, 42(1), 36–42. <https://doi.org/10.25100/socolen.v42i1.6667>
- Hall, D. G., & Hentz, M. G. (2011). Seasonal flight activity by the Asian citrus psyllid in east central Florida. *Entomologia Experimentalis et Applicata*, 139(1), 75–85. <https://doi.org/10.1111/j.1570-7458.2011.01108.x>
- Hernández, A. A., Giménez-Mujica, U. J., Hernández-Gracidás, C. A., & Oliveros-Oliveros, J. J. (2025). Optimizing control parameters for Huanglongbing disease in citrus orchards using SAIR-SI compartmental model, epidemic final size, and genetic algorithms. *Journal of Mathematical Biology*, 90(1), 4. <https://doi.org/10.1007/s00285-024-02161-1>
- Leong, S. S., Leong, S. C. T., & Beattie, G. A. C. (2021). Effect of horticultural mineral oil on Huanglongbing transmission by *Diaphorina citri* Kuwayama (Hemiptera: Psyllidae) population in a commercial citrus orchard in Sarawak, Malaysia, Northern Borneo. *Insects*, 12(9), 772. <https://doi.org/10.3390/insects12090772>
- Liu, Y., Gao, S., Chen, D., & Liu, B. (2024). Modeling the transmission dynamics and optimal control strategy for Huanglongbing. *Mathematics*, 12(17), 2648. <https://doi.org/10.3390/math12172648>
- Liu, Y. H., & Tsai, J. H. (2000). Effects of temperature on biology and life table parameters of the Asian citrus psyllid, *Diaphorina citri* Kuwayama. *Annals of Applied Biology*, 137(3), 201–206. <https://doi.org/10.1111/j.1744-7348.2000.tb00060.x>
- SAS OnDemand for Academics. 2021. https://www.sas.com/en_us/software/on-demand-for-academics.html. Accessed 2 Mar 2026.
- Singh, S., Sandhu, R. K., Sandhu, S. S., Gill, K. K., Siraj, M., Reddy, P. V. R., & Patil, P. (2024). Population prediction model of citrus psylla, *Diaphorina citri* Kuwayama on Kinnow Mandarin using weather data in Punjab, India. *Journal of Agrometeorology*, 26(2), 243–248. <https://doi.org/10.54386/jam.v26i2.2444>
- Wenninger, E. J., & Hall, D. G. (2007). Daily timing of mating and age at reproductive maturity in *Diaphorina citri* (Hemiptera: Psyllidae). *Florida Entomologist*, 90(4), 715–722. [https://doi.org/10.1653/0015-4040\(2007\)90\[715:DTOMAA\]2.0.CO;2](https://doi.org/10.1653/0015-4040(2007)90[715:DTOMAA]2.0.CO;2)
- Xie, F., Luo, Y., Zhang, Y., & Gao, S. (2025). High-dimensional modeling of Huanglongbing dynamics with time-varying impul